Algerian Journal of Environmental Science and Technology
June edition. Vol.8. N°2. (2022)
ISSN : 2437-1114
www.aljest.org

Mechanical and damage properties of polyethylene reinforced with clay treatment

B. Chebbab[1*], M. Djeziri[2,3], B. Bezzazi[1]

[1]Research Unit: Materials, Processes and Environment (UR/MPE), Faculty of technology,University M'hamed Bougara 35000 Boumerdes, Algeria.
[2]Center for scientific and technical research in Physico-chemical analysis (CRAPC) BP 384 Bouismail, Tipaza. Algeria.
[3]Research Laboratory in Food Technology, Faculty of technology, University M'hamed Bougara of Boumerdes 35000, Algeria.

*Corresponding author: b.chebbab@univ-boumerdes.dz

ARTICLE INFO

Article History:

Received ***: 01/05/2020***
Accepted ***: 30/10/2020***

Key Words:

Clay particles, chemical modifications, mechanical properties, SEM.

ABSTRACT/RESUME

Abstract: *This document is the subject of an experimental study for composite material implementation with a polyethylene matrix (HDPE) embedded with clay particles. We carried out a chemical optimization applied to clay particles by characterizing the mechanical behavior as well as the damage of the elaborated composite material. The work is based on the following optimized procedure: a mixture of sodium thiosulfate ($Na_2S_2O_3$) and clay cooled and centrifuged for 15 minutes. The clay pellet is rinsed twice with 0.05 M HCl for 3 to 4 hours. The mechanical properties of the composite material obtained are relative to the mass fraction of treated and untreated clay. The Young's modulus is found to change as the mass loadings of the injected treated clay change, with a marked improvement over virgin HDPE from 1590.90 to 1667.32 MPa, the yield strength from 28.68 to 31.73 MPa, and the ultimate tensile strength from 19.99 to 20.84 MPa. This positive variation is achieved at a maximum of 7% mass load of treated clay. Beyond this rate, the composite material experiences a drop in these same parameters due to the high concentration of clay. Scanning electron microscopy is used to see differences in dense microstructure between specimen granules.*

I. Introduction

The growing research interest in nanocomposites is giving this field a dynamic study and a perpetual evolution. This very active branch has found industrial applications, but these are still limited to a few types of materials. Polymer matrix and clay (bentonite) reinforced nanocomposites are given as the main applications to date. The natural clays to be extracted are prepared in nano reinforcements [1].

The use of polymers is controlled and inexpensive, which is why the development of organic matrix nanocomposites is highly developed compared to the ceramic or metallic matrix. The incorporation of clay particles is relatively proportional to its contact surface in the polymer for the same filler rate [2].

Polymer properties are modified by incorporating inorganic nanoparticles into the polymer matrix Ji-Zhao Liang [3], and (J Gonzalez-Benito et al.,[4]. Thus, the obtained nanocomposites would acquire new properties in terms of nature, shape, size, rate of introduced particles as well as the interface between the polymer and the nanoparticle.

In this context, a lot of work has been done from a morphological point of view such as : Cora O. Rohlmann et al.,[5] which studied the comparative analysis of polypropylene-based nanocomposites and different montmorillonites. They obtained nano-composite materials with intercalation and exfoliation with different percentages by weight of polypropylene, maleic anhydride modified polypropylene (PPg) and organophilic montmorillonites (OMMTs). (Xiaoyu Meng Zhe Wang et al.,[6] in turn treated the evolution of montmorillonites (OMMTs) with polyamide 12 (PA12) to see the factors that influence the nano composites. The exfoliated mixture obtained is proportional to molecular weight.

Contrary to the morphology, we note that AD Drozdov J de C Christiansen [7] have studied nano composites based on polyethylene matrix (HDPE) and clay from the mechanical point of view such as: Uni-axial cyclic traction with different speeds ranging from 1 to 50 mm/min. The experimental result obtained gave a model responding to the viscoplasticity of the polymers with three-dimensional cyclic deformations at small deformations. The results obtained are adequate with numerical simulation.

The work carried out by (Rund Abu-Zurayk et al.,[8] on biaxial deformation of polypropylene-clay nanocomposites under industrial forming conditions to determine whether the presence of clay affects the transportability, structure and mechanical properties of the stretched material. The results obtained show that the presence of clay increases the yield strength compared to unfilled material at typical processing temperatures and that the sensitivity of the yield strength to temperature is greater for the filled material.
In this work, nano-composite polymers were developed by incorporating nano-sized clay nanoparticles of nano scale diameter into a matrix of HDPE grade 4903. The presence of clay nanoparticles affects the mechanical and structural properties of nano-composite polymers, which we present experimentally in the following.

II. Materials and methods

II.1. Thermoplastic preparation

HDPE (Grade 4903) is a semi-crystalline thermoplastic widely used in engineering applications such as piping and pressure vessels. HDPE (Grade 4903) is a product marketed by the National Company of the Petrochemical Industry ENIP (Algeria) in the form of 3 to 4 mm diameter aggregates, packed in 50 kg bags. The technical and physical specifications of the thermoplastic materials of this high-density polyethylene, are grouped in the table 1.

Table 1. *HDPE characteristics Grade 4903.*

Characteristics of HDPE Grade 4903	Standard	Values
Density	ASTM D1505	0.950 g/cm
Melt flow index	ASTM D1238	0.2à1.4g/10 (min)
Crystallinity rate	-	70%
Melting temperature	-	190 °C
grains number /	MA-55-3011	30-40 grains/gr

This HDPE (Grade 4903) will be ground to obtain fine particles that will be mixed with the treated and untreated clay.

Figure 1a*. HDPE Grade 4903 (aggregates form).*

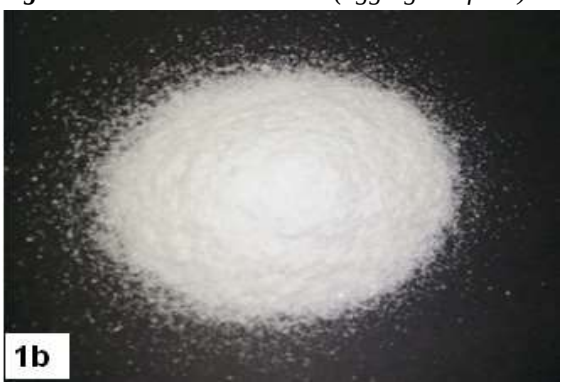

Figure 1b. *Ground HDPE Grade 4903.*

II.2. Clay preparation and extraction

The clay we used is a drilling bentonite taken from the Hammam Boughrara (Maghnia) West Algeria deposit. The sample taken underwent the following preliminary unit operations :

- Crushing of bentonite rocks into pieces.
- Drying in an oven at 80°C for 24 hours.
- Grinding of the bentonite pieces in a shank mill until the grain size of a nano scale value is obtained.

II.3.Particle size analysis by laser diffraction

The powder particle size distribution was determined by static light scattering using a Malvern Mastersizer S particle size analyzer (Malvern Instruments Ltd, UK). This type of instrument is equipped with an He/Ne laser with a power of 5 mW at a wavelength of 632.8 nm. A particle scatters the light at an angle inversely proportional to its size. Larger particles deflect a larger amount of light at smaller angles and vice versa for smaller particles. Data acquisition is performed using Malvern processing software (Sizer Sv2.17).

II.4. DRX identification of structural phases

The crystalline phases were identified by X-ray powder diffraction using a Brüker D5000 diffractometer with a graphite rear monochromator, operating at 40 kV voltage and 50 mA current with CuKα radiation as the radiation source and controlled by a computer with Diffracplus D software version 2.2.

II.5. Infrared Analysis (IFTR)

The apparatus used is an Alpha Fourier Transform spectrophotometer from Bruker . The spectrum analysis is performed in the 4000-400 cm^{-1} wave number range (64 scans, resolution $1cm^{-1}$).

II.6. Thermal analysis by DSC, ATG

The tests were carried out on a DSC SDT 600 TA Instrument performing two runs (CARIN, A 2002): the first is performed to overcome the thermal history of the materials; the second allows the measurement of different transitions in the foods studied. The heating and cooling rates are set at 10°C/min, with a flow rate of 100 ml/min of nitrogen. Samples with a mass of 5 mg are placed in an aluminium crucible sealed with a deep-drawn lid. An empty crucible of the same weight is used as a reference. The apparatus is calibrated in temperature and power with a sample of indium of known temperature and enthalpy of fusion: Tf = 156,6°C and ΔHf = 28,4J/g.

II.7. Chemical treatment of clay particles

120 grams of bentonite are dispersed in a 5 litre beaker containing 1.5 litres of distilled water. The mixture obtained is kept under stirring for 15 minutes. A buffer solution (0.3 M sodium citrate, 1M sodium bicarbonate and 2M sodium chloride) is then added at pH=7.3.

The mixture is heated under stirring at a temperature of 75°C for 15 to 20 minutes. Then 15 grams of sodium thiosulphate ($Na_2S_2O_3$) are added and after 15 minutes of stirring, 15 grams of ($Na_2S_2O_3$) and 1% CTAB are added. The cooled mixture is centrifuged at 6000 rpm for 15 minutes. The bentonite pellet is washed twice with HCl at 0.05 M (1.5 L) for 3 to 4 hours. After centrifugation, the bentonite is dispersed in 2.5 L of hydrogen peroxide (H_2O_2: 10 volumes) overnight, then heated at 70°C for 30 min to remove organic matter (a quantity of Fe2+ could oxidize to Fe3+).The purified sample is washed 3 times with a 0.3M NaCl solution. Sodium bentonite is obtained by ion exchange. Disturbing Cl- ions are removed by successive washing with water. A silver nitrate (AgNO3) test confirms the absence of Cl- ions. The fraction of bentonite with a particle size of less than 1 micron is collected by sedimentation after 8 hours, as the heavier particles (impurities) sediment faster (Stockes' law). After centrifugation at 3500 rpm, the collected montmorillonite -Na+ is dried in an oven at a temperature of 40°C for 3 days, then stored in a vacuum desiccator for later use.

Figure 2a. *Clay particles. before treatment.*

Figure 2b. *Clay particles after treatment.*

II.8. Composite (HDPE+Clay) Method of Making Composite Material

II.8.1. Mixing HDPE / Clay in an internal mixer.

The products are dried in an oven at 80°C for 04 hours to completely remove moisture and then placed in a vacuum desiccator.

Melt mixing is carried out using a Brabender Gmbh & Co.KG internal mixer. Equipped with Mixer data correlation acquisition software, this device allows the

measurement of the torque induced by the material which reflects the rheological behaviour of the mixture present in the chamber (Figure 3). It has a 50-gram capacity chamber in which two counter-rotating blades move. The maximum temperature set point is set at 190°C. The material temperature is measured by means of a thermocouple placed in the chamber. The motorisation allows a maximum rotation speed of 50 rpm for 10 minutes. The maximum torque is 58 Nm; it should be noted that the torque is not measured using a sensor, but calculated from the induced current.

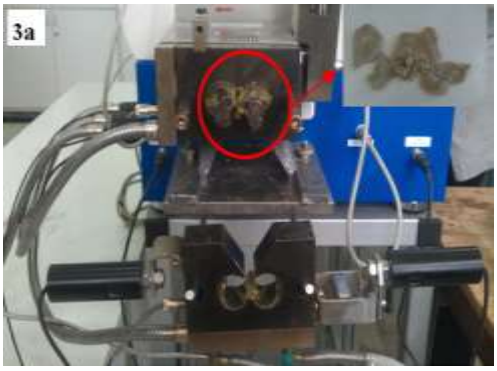

Figure 3a. *The mixing chamber*

Figure3b. *Material recovered after mixing.*

II.8.2. Preparation of HDPE+Clay specimens by the extruder and the press

All the mixtures thus produced will be crushed and then moulded in a twin-screw corotative extruder DSM Xplor Netherlands of 15 Cm^3 at 190°C with a rotation speed of 100 rpm for 4 minutes.

Tensile test specimens (ISO 527-2 1BA standard) were injected using an injection moulding machine (Xplor Injection Moulding Machine) at a temperature of 190°C with a pressure of 10 bar.

Figure 4a. *Preparation of specimens, mini corotating twin-screw extruder DSM Xplor Netherlands 15 Cm^3.*

Figure 4b. *Press (Xplor injection Moulding Machine).*

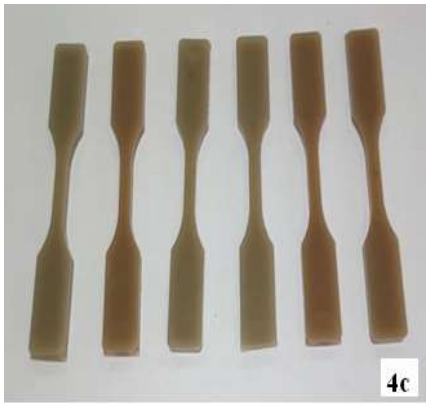

Figure 4c. *HDPE / Clay test tubes.*

II.9. Composite Characterization

II.9.1. Tensile Test

The specimens are prepared according to ASTM D3039. These meet the requirements of the tensile test conditions. The tensile tests were carried out in accordance with ASTM D-638M designation with a speed of 2mm/min at room temperature on a Zwick / Roell Z010 universal tensile machine at the UR-MPE research unit, equipped with a 10 kN capacity force transducer. This machine is computer-controlled using TextXpert 12.0 software.The values of Young's modulus, maximum elastic stress and strain at break are determined for each type of specimen for the

different mass fractions of the clay. For each type of composite material (Table 2), five specimens were tested. The values of Young's modulus, yield strength, stress and strain at break are determined for each specimen.

Table 2. *Different loads for composite material with their designations.*

Materials	Designation
Polyethylene pure	PEHD
Polyethylene charged with 3% clay Untreated	PEHD/Clay Untreated3%
Polyethylene charged with 7% clay Untreated	PEHD/Clay Untreated7%
Polyethylene charged with 3% clay treated	PEHD/Clay Treated 3%
Polyethylene charged with 7% clay treated	PEHD/Clay Treated 7%
Polyethylene charged with 10% clay treated	PEHD/Clay Treated 10%

Figure 5. *Mechanical tensile test photo.*

II.10. Scanning electron microscopy (SEM)

The observation of the powder microstructure was carried out using scanning electron microscopy (SEM-EDX Quanta 250 with tungsten filament from the FEI company). The dry powder was deposited on an adhesive and conductive observation support and then metallized by argon plasma. The observation was carried out under vacuum at an accelerating voltage of 15 kV. (Energy Dispersive Spectroscopy).

III. Results and Discussion

III.1. Particle size analysis by laser diffraction

The particle size distribution of the clay powder is shown in Figure 6.

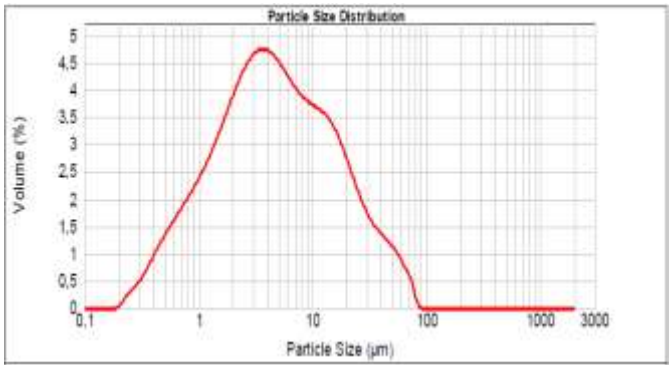

Figure 6. *Particle size distribution (by volume) of the clay.*

The results show that the particle size distribution is trimodal for the clay powder. For the studied powder the largest proportion of particles is around 24.15 µm see (fig. 6). The parameters d10, d50 and d90 were determined by the software see table 2. They represent the size below which 10, 50, 90 % of the population is found in volume. The criterion d10 characterizes small particles while d90 characterizes large ones. The values of d10 d50 and d90 for powders differ significantly and are on average 0.872, 4.511 and 24.14 mm respectively.

Table 3. *Data collected from the laser granulometry curves.*

Characteristics	Powder
d (V; 0.1) (increasing to 10%) µm	0.872
d (V; 0.5) (median diameter) µm	4.511
d (V; 0.9) (increasing to 90%) µm	24.146
Span (distribution width) = (D90-D10)/D50	5.160
Concentration % vol	0.0001
Uniformity	1.64
Specific surface area (m2/g)	2 .72
Mean diameter (Volume) D (4;3) in µm	9.441
Weighted average diameter D (3;2) in µm	2.207

Table 3 shows the main results of the physical characterization of the clay powder. The diameters d10, d50 and d90 are determined using the Mastersizer 2000 (Malvern Instrument) laser particle size analysis under wet conditions. The flow velocity of the suspension in the circuit as well as the ultrasonic time are parameterized to optimize the dispersion of the particles. The solid concentration of the suspension is limited to avoid measurement errors induced by the occurrence of multiple scattering phenomena. Due to the mineralogical heterogeneity of the materials under study and the birefringent character of bentonite, the

calculation of an average refractive index seems highly random. The size distributions were therefore calculated using the Fraunhoffer approximation. The low values of the median diameters d50 obtained (less than 5 µm) suggest that significant measurement errors could affect the fine fraction of the size distribution. This remark would then explain the low dispersion of the measured d10 (all between 0 and 1 µm). It can be seen that the clay powder is characterized by a specific surface area of between 2 and 3 m2 /g.

III.2. DRX identification of structural phases

The determination of the clay structural phases used in our study by X-ray diffraction is given in figure 7.

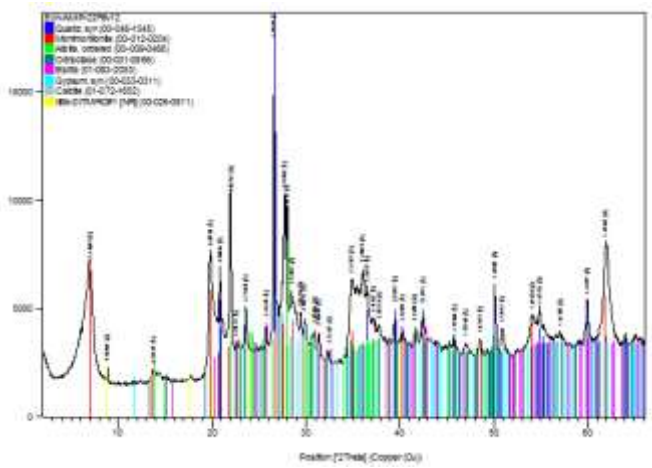

Figure 7. *The X-ray diffractogram of the clay.*

This latter reveals that our clay is essentially made up of, in decreasing order, several crystalline phases which are of majority phase Quartz ≈ 30%, Montmorillonite ≈ 30%, Orthoclases ≈ 16%, Albite ≈ 13%, Barite ≈ 3%, Calcite ≈ 3%, Illite ≈ 2%, Gypsum ≈ 1%. It mainly reveals the presence of four intense peaks, the first and fourth correspond to Montmorillonite alone and the other two to a mixture of Quartz, montmorillonite and albite, which implies that our clay is heterogeneous. Our results are in perfect agreement with those obtained by Qlihaa A et al.,[9] who worked on a raw Moroccan clay.

III.3. Infrared Analysis (IFTR)

Fourier Transform Infrared Spectroscopy (FTIR) is a reliable reference technique for studying the intra- and intermolecular interactions of a material. It has been performed to identify functional groupings of the material being processed. Figure 8 shows the FTIR spectrum of the specimen formulated from clay and the polymer.

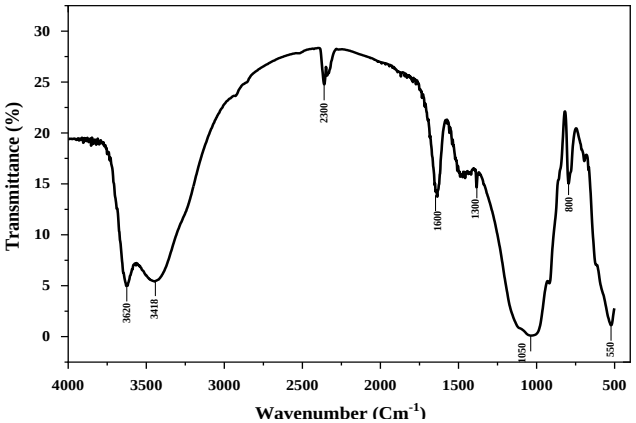

Figure 8. *FTIR spectrum of the elaborated specimen.*

The spectrum obtained for the specimen analysed shows marked differences at wavelengths of 3620, 3418, 2300, 1628, 1050 and 550 Cm^{-1}. The peaks obtained at 3620 and 3418 Cm^{-1} would correspond to the symmetrical and asymmetrical vibrations of water, which can be weak for granules during drying [10], whereas the peak obtained at 2300 and 1628 Cm^{-1} would correspond to the C=O elongation vibrations of the carboxyl groups [11]. The other spectra show absorption corresponding to wavelengths 571, 1018, 1023, 1149 and 1455 Cm^{-1} confirming the clayey nature of the sample.

The spectrum shows different regions [12, 13].

- Region of vibration of hydroxyl groups: between 3700 and 3400 Cm^{-1} for the valence vibration bands. Between 900 and 600 Cm^{-1} for angular deformation bands.
- Vibration region of the silicate anion: between 1200 and 700 Cm^{-1} for the valence vibration bands. Between 600 and 400 Cm^{-1} for the deformation bands.

Vibration region of the hydration water of the interfoliar cations: the valence vibration bands are between 3640 and 3400 Cm^{-1} and are superimposed on the OH valence bands of the clay network. The deformation bands are between 1650 and 1610 Cm^{-1}.

The vibrations, appearing on this spectrum and recorded between 4000 and 400 Cm^{-1}, can be attributed as follows: The spectrum of the specimen shows bands between: 3200-3700 Cm^{-1} attributed to the O-H elongations of the structural hydroxyls. We distinguish, for the analyzed sample, a band at 3600 Cm^{-1} corresponds to the internal OH groups of the octahedral layer and that at 3418 Cm^{-1} to the water of hydration. The band situated around 695 Cm^{-1} on the spectrum reveals the presence of kaolinite [14]. We distinguish, also for a band located between 1620 and 1630 Cm^{-1} corresponds to H_2O deformation vibrations. Another band at 800 Cm^{-1} attributed to halloysite [15]. The Si-O valence vibrations are in the form of a shoulder at 1120 Cm^{-1} and a band at 1050

Cm^{-1} respectively. The lattice deformations are between 400 and 580 Cm^{-1} for the Si-O and Si-O-Fe and Si-O-Al bands. We note the presence of the 1300 Cm^{-1} band attributed to calcite and the quartz band at 2300 Cm^{-1} [16]. These results are in agreement with those found from DRX. They confirm the presence of Quartz, Kaolinite and Illite in the clay studied.

III.4. Scanning electron microscopy (SEM) The identification of the specimen structure by SEM (scanning electron microscopy) is shown in figure 9.

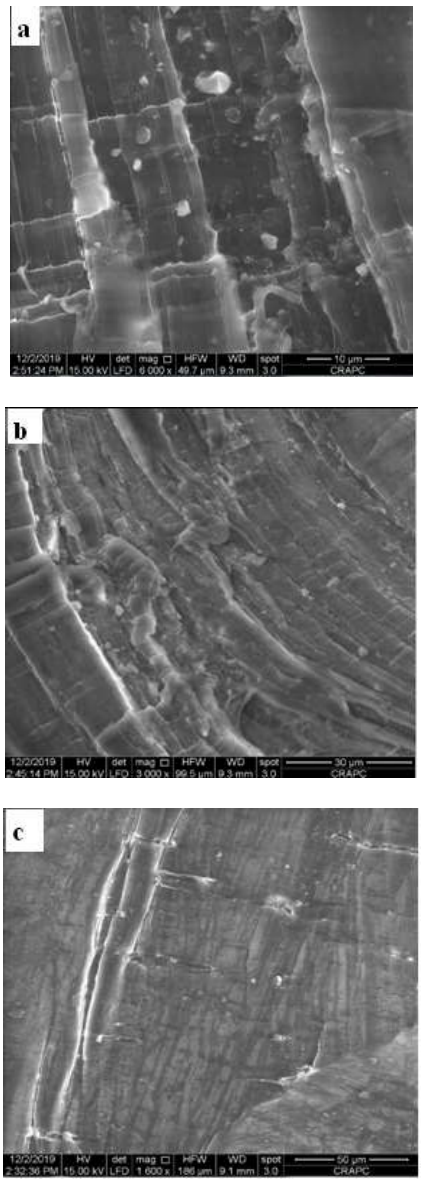

Figure 9. *Scanning electron microscopy (SEM) images analysis.*

The observations (Figure 9) reveal dense microstructural differences between specimen granules. In fact, we observe in the sample the presence of irregular surfaces in the form of juxtaposed blades of clay [17]. On the other hand, the sample also presents a microporous structure of the order of 1.5 µm pore diameter [18]. Our results are similar to those obtained by A J M S Lim et al., [19] , that they worked on a clay from Malaysia which they worked on a clay from Malaysia, and they found irregular and microporous surface structures.

III.5. Thermal analysis by DSC, ATG
The thermal transitions of the sample analyzed by differential thermal analysis are shown in Figure 10.

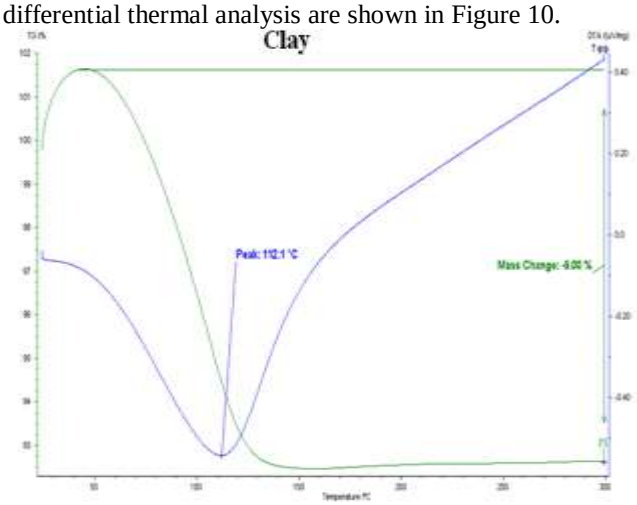

Figure 10. *Thermal analysis of clay.*

The sample shows a thermogram with a simple endothermic transition typical of the drying process [20].

Table 4. *Data collected from GTA/DSC curves.*

Sample	DSC parameters					ATG parameters
	T_0 (°C)	T_p (°C)	T_c (°C)	T_c-T_0 (°C)	ΔH (J/g)	Masse Change
Clay	34.40	112.10	170.00	135.60	-	9

T_0 = Drying start temperature; T_p = Peak temperature; T_c = End temperature. ΔH= Transition enthalpy.

The results of the differential thermal analysis carried out on the clay show an energy absorption by the sample accompanied by a loss of mass between 50°C and 150°C. This phenomenon is attributed to the departure of the "zeolitic" water. Heating to 105°C is therefore not sufficient to evacuate all the water from the clay, which still benefits from the cohesion

provided by microscopic capillary bridges between the clay plates.

The effects observed on the thermal transition parameters (To, Tp, Tc, Tc-To and H) suggest that the variety of clay affects the overall molecular properties of the clay granules, although only one % clay was used. An increase in Tp could result from the weakening of the granules affected by the modification (drying) [20], which is consistent with our spectroscopic observations of the clay. The percentage by weight of this loss calculated according to the TGA curve is of the order of 9%, this important rate is mainly due to the important percentage of the fine fraction in this clay and corresponds to a dehydroxylation of the clay [21].

III.6. Temperature evolution

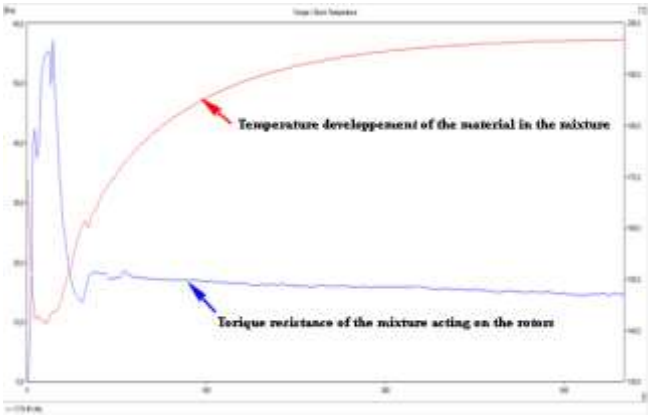

Figure 11. *Temperature development of the material and torque resistance of the mixture acting on the rotors.*

On red curve we observe a first temperature drop in relation to the set temperature, due to the introduction of the polymer at room temperature into the chamber. This temperature will drop conspicuously due to the introduction into the chamber of the mixture of HDPE and clay which is at room temperature. As the PC softens, it will increase its temperature to reach a steady state at the temperature set at the beginning. The variation of this temperature is therefore quite important and has several origins :

- Introduction of the material at room temperature;
- Friction of the rotors on the pellets, viscous dissipation;
- More or less efficient regulation system.

III.7. Evolution of the torque

The blue Curve shows the increase in torque, reflecting the friction of the granules which, under thermal and mechanical action, will soften and then interpenetrate to form a homogeneous medium. The torque then reaches a maximum speed, resulting in a drop in torque, is observed. However, the mixing action leads to a homogenization of the medium translated by the torque towards a constant equilibrium value.

III.7.1. Tensile Test

Figure 12 shows the plot of stress versus strain for virgin polyethylene and HDPE/clay composite material. The mechanical properties of the composite material obtained are relative to the mass fraction of treated and untreated clay. The Young's modulus is found to change as the mass loadings of the injected treated clay change, with a significant improvement over virgin HDPE from 1590.90 to 1667.32 MPa. There is also an improvement in yield strength from 28.68 to 31.73 MPa and in ultimate tensile stress from 19.99 to 20.84 MPa. This positive change is achieved at a maximum of 7% mass loading of the treated clay. These positive results show that there was a good distribution of clay in the matrix from which we conclude a good interfacial adhesion of the clay with the polyethylene. This is due to the respect of the clay treatment procedure (rinsing by HCl at 0.05 M, centrifugation, purification by NaCl at 0.03 M and the demonstration of the presence of chloride by silver nitrate ($AgNO_3$), i.e. purification. The mixing (HDPE - Treated Clay) is carried out in a Brabender Gmbh & Co.KG internal mixer at a standardised melting temperature of 190°C.

Above this rate, the composite material experiences a drop in these same parameters due to the high concentration of clay.

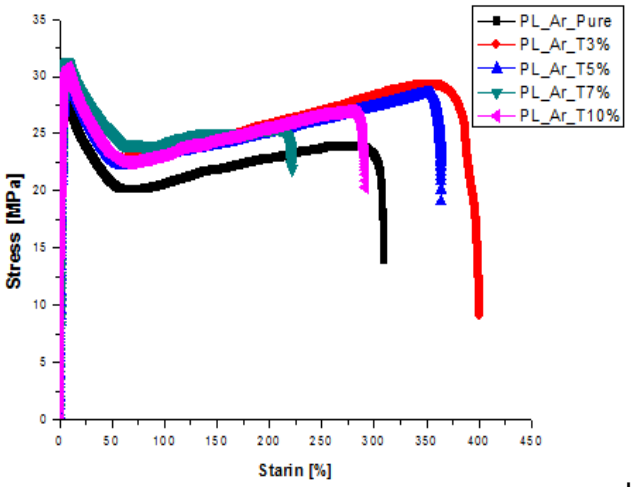

Figure 12. *Stress-Strain curve of Polyethylene reinforced with deferent's volume fraction of treated clay.*

Algerian Journal of Environmental Science and Technology
June edition. Vol.8. N°2. (2022)
ISSN : 2437-1114
www.aljest.org

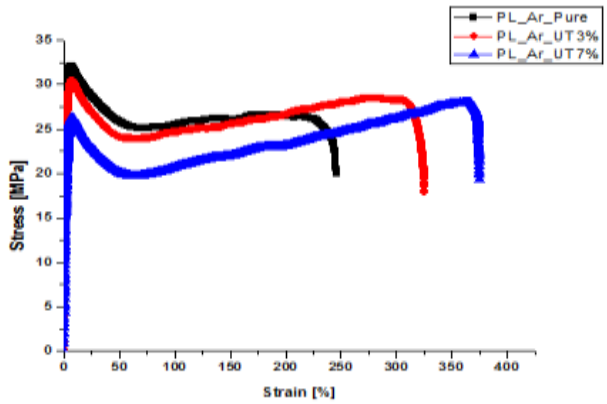

Figure 13. *Stress-Strain curve of Polyethylene reinforced with deferent's volume fraction of untreated clay.*

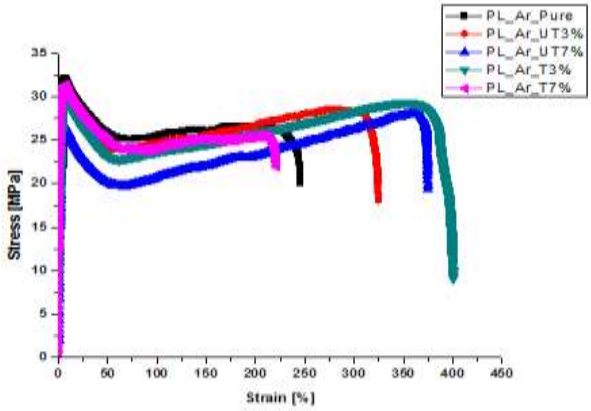

Figure 14. *Stress-Strain curve of Polyethylene reinforced with deferent's volume fraction of treated and untreated clay.*

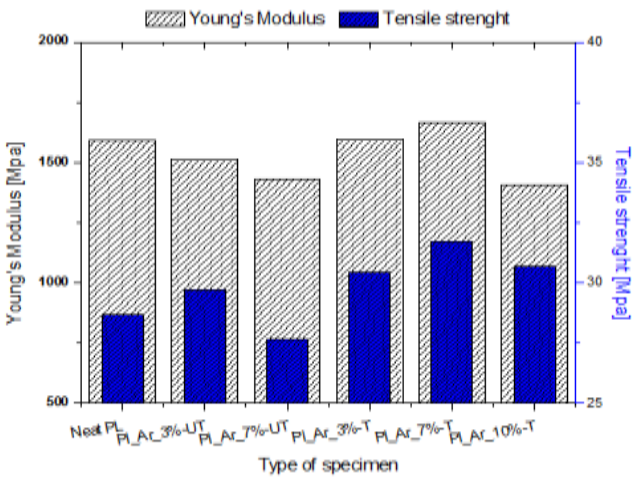

Figure 15. *The evolution of Young's modulus as a function of the volume fraction of processed and unprocessed feedstocks.*

Table 5. *Main value of mechanical properties for different types of composite with treated and untreated clay, n number of specimens.*

Materials	Tensile modulus (MPa)	Tensile strength (MPa)	Breaking Stress (MPa)	Breaking Strain (%)	n
virgin PEHD	1590.90 ±24.56	28.68 ± 0.08	19.99 ±01.53	245.76 ±26.43	5
PEHD/Clay _3%-T	1594.86 ±80.49	30.43 ± 0.92	18.98 ±01.04	325.20 ±22.86	5
PEHD/Clay _7%-T	1667.32 ±75.94	31.73 ± 1.72	20.84 ±01.96	374.59 ±13.25	5
PEHD / Clay _10%-T	1405.4 ±15.84	30.7 ± 0.72	21.04 ±01.96	278.76 ±26.43	5
PEHD / Clay _3%-UT	1511.67 ±18.67	29.70 ± 0.37	09.66 ±01.05	464.64 ±83.26	5
PEHD / Clay _7%-UT	1429.55 ±01.24	27.64 ± 0.55	22.19 ±03.59	221.34 ±43.25	5

Table 6. *Percentage improvement of different types of composite by Neat HDPE, HDPE/Clay_V% untreated Clay.*

Types of specimen	Tensile modulus (MPa)	Improvement (%)
Vergin HDPE	1590.90 ± 24.56	100
HDPE / Clay _3% -T	1594.86 ± 80.49	100.25
HDPE / Clay _7% -T	1667.32 ± 75.94	104.80
HDPE / Clay _10% -T	1405.4 ± 15.84	88.34
HDPE / Cay_3% - UT	1511.67 ± 18.67	95.02
HDPE / Cay_7% - UT	1429.55 ± 01.24	89.86

IV. Conclusion

The characteristics of the composite material obtained by the tests showed that there is a good dispersion of the clay particles in the matrix, resulting in a better cohesion of the clay particles with the polymer. The clay was treated by introducing 1% of CTAB (Cethyl trimethyl ammonium bromide), this contributed to the strengthening of the clay in the matrix. The result obtained by the SEM confirms a uniform dispersion of clay particles in the polymer. Knowing that the composite obtained HDPE and clay had an improvement in Young's modulus from 1590.90 to 1667.32 MPa, this result shows the performance of the reinforcement of the composite material at a determined clay mass percentage (7%), because by exceeding this percentage we see a perversion of the Young's modulus.

V. References

1. Dantas de Oliveira, A. ; Augusto Gonçalves, Beatrice C. Polymer Nanocomposites with Different Types of Nanofiller. Nanocomposites, *Recent Evolutions*, (2019) doi: http://dx.doi.org/10.5772/intechopen.81329.
2. Kerstin, M. ; Elodie, B. ; Marcos, L. ; Maria, J.; Yolanda, E. ; Sanz José, M. ; Lagaron Oliver, M. ; Alvise, B. ; Steve, H. ; Uwe, B. ; Germán, P. ; Marius, J. ; Martina, L. ; Zuzana, S. ; Sara, C. ; and Markus, S. *Review on the Processing and Properties of Polymer Nanocomposites and Nanocoatings and Their Applications in the Packaging, Automotive and Solar Energy Fields*, Nanomaterials 7 (2017) 74.
3. Liang, J.Z. Reinforcement and quantitative description of inorganic particulate-filled polymer composites. *Composites Part B* 51 (2013) 224-232.
4. Gonzalez-Benito, J. ; Martinez-Tarifa, J. ; Sepúlveda-García, M.E. ; Portillo, R.A. ; Gonzalez-Gaitano, G. Composites based on HDPE filled with $BaTiO_3$ submicrometric particles. Morphology, structure and dielectric properties. *Polymer Testing* 32(2013) 1342-1349.
5. Rohlmann, C.O. ; Fernanda, M. ; Horst, L. ; Quinzani, Marcelo, M. ; Failla, D. Comparative analysis of nanocomposites based on polypropylene and different montmorillonites » *European Polymer* Journal 44 (2008) 2749–2760.
6. Xiaoyu, M.; Zhe, W.; Zhongfu, Z. ; Xiaohua, D. ; Wuguo, B.; Tao, T. Morphology evolutions of organically modified montmorillonite/ polyamide 12 nanocomposites » *Polymer* 48 (2007) 2508 –2519.
7. Drozdov, A.D. ; Christiansen, J.C. Cyclic viscoplasticity of high-density polyethylene/montmorillonite clay nanocomposite . *European Polymer* Journal 43 (2007) 10–25.
8. Abu-Zurayk, R. ; Harkin-Jones, E. ; McNally, T. ; Menary, G. ; Martin, P. ; Armstrong, C. Biaxial deformation behavior and mechanical properties of a polypropylene/clay nanocomposite. *Composites Science and Technology* 69 (2009)1644–1652.
9. Qlihaa A. ; Dhimni, S. ; Melrhaka, F. ; Hajjaji, N. ; Srhiri, A. Caractérisation physico-chimique d'une argile Marocaine. *J. Mater. Environ. Sci*. 7 (5) (2016) 1741-1750.
10. Pelletier, M.; Thomas, F.; de Donato, P.; Michot, LJ. ; and Cases, JM. Infrared spectroscopic study of water vapor adsorption desorption by homoionic montmorillonites. The bending mode. In Clays for our future. Proceedings of the 11th International Clay Conference, Ottawa Canada. Kodama, H., Mermut, A.R., *Torrance, J.C.* (Eds). (1999a) ; 555-560.
11. Pezolet, M. ; Bonenfant, S., Dousseau, F., and Popineau Y. Conformation of wheat gluten proteins—Comparison between functional and solution states as determined by infrared spectroscopy. *FEBS Lett* 3(1992)247-250.
12. Srasra, E. Argile et acidité. Mécanisme de l'activation acide et propriétés résultantes. Thèse de Doctorat d'état en sciences physiques. (2002) Tunis.
13. Jahouach, W. Etude des propriétés physico-chimiques des huiles d'olive et de grignons d'olives décolorées par des argiles tunisiennes activées aux ondes ultrasonores. Thèse de Doctorat Sfax. (2012) Tunisie.
14. VD. Manuel Boutelspacher. Atlas of IR of clay minerals andtheir admixture, Elsevier scientific Publishing Company, Amesterdam, Oxford, New York.(1976).
15. Mellouk, S. ; Cherifi, S. ; Sassi, M. ; Marouf-Khelifa, K. ; Bengueddach, A. ; Schott, J. ; Khelifa, A. Intercalation of halloysite from Djbel Debagh (Algeria) and adsorption of copper ions. *Appl. clay sci* 44 (2009) 230-236.
16. Wilson, M.J. Clay mineralogy: Spectroscopic and chemical determinative methods, first. *Ed. Chapman. and Hall*. London (1995).
17. Houben, M.E. In situ characterization of the microstructure and porosity of Opalinus Clay (Mont Terri Rock Laboratory, Switzerland). *Faculty of Georesources and Materials Engineering.* The RWTH Aachen University, Germany. (2013).
18. Porfirio, M. ; Oisy, C.N. ; Raydel, H. ; Reinaldo, L. ; Borges, C. ; Caicedo, B. Study of the relationship between the hydromechanical soil behavior and microstructure of a structured soil. *Earth Sci. Res. J*. Vol 22 No. 2(2018)91-101.
19. Lim, A.J.M.S.; Syazwani, R.N.; Wijeyesekera, D.C. Impact of Oriented Clay Particles on X-Ray Spectroscopy Analysis. *Soft Soil Engineering International Conference* (2015) (SEIC2015).
20. Biliaderis, C.G. ; Zawistowski, J. Viscoelastic behavior of aging starch gels: effects of concentration, temperature and starch hydrolyzates on network properties. *Cereal Chem* 67(1990)240-246.
21. Tomasik, P.; Zaranyika, MF. Nonconventional methods of modification of starch. *Adv. Carbohydr. Chem. Biochem*. 51 (1995) 243–318.

Please cite this Article as:
B. Chebbab., M. Djeziri., B. Bezzazi., Mechanical and damage properties of polyethylene reinforced with clay treatment, ***Algerian J. Env. Sc. Technology***, **8:2 (2022) 2409-2418**